SCIENTIFIC OASIS

Spectrum of Mechanical Engineering and Operational Research

Journal homepage: www.smeor-journal.org
ISSN: 3042-0288

Modeling Uncertainty in Engineering Problems Using Asymmetric Interval Numbers (AINs)

Szymon Śniegowski[1], Adrianna Świder[2], Andrii Shekhovtsov[1,2], Wojciech Sałabun[1,2,*]

[1] National Institute of Telecommunications, Warsaw, Poland
[2] West Pomeranian University of Technology in Szczecin, Szczecin, Poland

ARTICLE INFO

Article history:
Received 11 August 2025
Received in revised form22 September 2025
Accepted 23 October 2025
Available online 27 December 2025

ABSTRACT

Engineering systems are increasingly complex and subject to multiple sources of uncertainty arising from geometric tolerances, material variability, and operating conditions, which significantly affect performance and reliability, making accurate modeling of uncertainty essential in modern engineering analysis. Classical interval analysis is a well-established approach for representing uncertainty; however, traditional interval numbers (CINs) assume a symmetric and uniform distribution around the central value, whereas in practice, uncertainties are often asymmetric due to uneven measurement errors, technological deviations, or differing consequences of overestimation and underestimation. As a result, symmetric intervals may distort risk assessment and reduce the accuracy of results. This study introduces Asymmetric Interval Numbers (AINs), a generalization of classical interval numbers that allows independent modeling of uncertainty in the positive and negative directions. AINs provide a more realistic and flexible framework for representing asymmetric data distributions while retaining the simplicity of interval analysis. To demonstrate their applicability, three case studies involving different classes of engineering problems were conducted, and the results show that AINs improve the realism, stability, and interpretability of uncertainty modeling compared with classical interval approaches, confirming their potential as an effective tool for engineering analysis.

Keywords:
Asymmetric Interval Numbers; AINs; Uncertainty Modeling; Engineering Analysis

1. Introduction

Modern engineering systems are characterized by increasing complexity and numerous sources of uncertainty arising from geometric tolerances, material property variability, and operating conditions [1, 2]. The influence of these factors significantly affects the performance and reliability of designed

*Corresponding author.
E-mail address: W.Salabun@il-pib.pl

https://doi.org/10.31181/smeor31202651

solutions, and their omission may lead to incorrect assessments or even system failures. Therefore, precise modeling and quantification of uncertainty have become key components of modern engineering analyses [1].

One of the classical approaches to representing uncertainty is interval analysis, the fundamentals of which were developed by Ramon E. Moore [3]. Despite its wide acceptance and long history of applications, the classical interval numbers (CINs) used in this approach have significant limitations [4, 5]. They assume a symmetric and uniform distribution around the central value [3], which often does not reflect real-world data, where uncertainty tends to be asymmetric [6]. In engineering and experimental practice, distributions of measurement errors, technological deviations, or input parameter variations are rarely symmetric [7, 8]. In many cases, such as structural safety assessment or material durability evaluation, the consequences of overestimating versus underestimating admissible values carry completely different significance. Accounting for this asymmetry is therefore essential to accurately reflect the actual level of uncertainty and to improve the quality and reliability of analytical results. The use of symmetric intervals in such cases may distort risk assessments, reduce result precision, and create additional computational challenges [4, 9]. In response to these limitations, a new class of numbers, Asymmetric Interval Numbers (AINs), has been proposed as a generalization of classical interval numbers. AINs allows for the independent modeling of uncertainty in the positive and negative directions relative to the central value, enabling a more realistic representation of asymmetric data distributions. This, in turn, makes it possible to more accurately capture phenomena in which the level of risk or error is not the same on both sides of the interval, thereby significantly extending the applicability of interval analysis in engineering and applied sciences [4].

With the advancement of research on engineering systems, it has become increasingly apparent that different groups of methods used to represent uncertainty possess both advantages and limitations [10, 11]. Classical probabilistic approaches are based on the assumption that input variables can be described by known probability distributions, allowing for accurate analysis when a sufficient amount of data is available [12]. In practice, however, obtaining reliable statistical information is often difficult or even impossible, which limits the scope of their application [13]. Although methods based on interval analysis, fuzzy models, or evidence theory are capable of representing uncertainty with limited input data, they often lead to overly conservative results or a loss of information regarding the structure and direction of that uncertainty [14].

In this context, Asymmetric Interval Numbers represent an intermediate approach that combines the advantages of interval and probabilistic methods. They enable flexible modeling of asymmetric uncertainty while maintaining formal simplicity and computational efficiency, making them applicable to a wide range of engineering problems.

To illustrate the practical potential and applicability of AINs, three case studies have been developed, covering different classes of problems where input data uncertainty plays a crucial role. Each case represents a distinct modeling context, from energy estimation to aerodynamic interaction analysis, allowing for a comparison between the results obtained using AINs and those based on CINs. The results of these analyses confirm that applying AINs leads to more realistic, stable, and interpretable outcomes, highlighting their potential as a universal tool for uncertainty analysis in engineering applications.

The remainder of this paper is organized as follows: Section 2 presents the theoretical foundations of AIN concept and its relationship to CIN. Section 3 describes the implementation of the proposed approach and the computational procedures used. Section 4 introduces three case studies illustrating practical applications of AINs in engineering analyses and compares their results with CINs, and Section 5 provides a summary of the findings and outlines directions for future research.

2. Realted works

In recent years, the field of uncertainty quantification in engineering has experienced dynamic growth. Intensive research has focused both on improving classical probabilistic and non-probabilistic methods and on integrating them with modern artificial intelligence techniques. Such approaches are finding increasingly broad applications across various areas of engineering.

In the literature, various Bayesian methods have been extensively developed and applied to uncertainty quantification in engineering. Pasparakis et al. [15] employed Bayesian neural networks to predict full-field material responses, enabling the representation of both epistemic and aleatory uncertainty. Abulawi et al. [16] proposed the Bayesian Optimized Deep Ensemble method, which improves the calibration of confidence intervals in deep learning model predictions, illustrated through the modeling of thermohydraulic phenomena in a sodium-cooled reactor. On the other hand, Ochella et al. [17] utilized Bayesian neural networks to predict the remaining useful life of sensor-monitored systems, demonstrating that integrating Bayesian methods with machine learning enables realistic uncertainty quantification in engineering forecasts. A further development of the Bayesian framework was presented by Kurumbhati et al. [18], who applied Hierarchical Bayesian Models (HBM) to the calibration of constitutive parameters in the Giuffré–Menegotto–Pinto (GMP) model for reinforcing steel. Their analysis was based on data from 36 steel coupons subjected to cyclic stress–strain tests from various mills and manufacturing standards. Unlike classical approaches limited to epistemic uncertainty, HBM enables the simultaneous modeling of aleatory variability arising from sample-to-sample differences. The resulting a posteriori distributions of material parameters allow for more reliable uncertainty propagation and can be applied to structural reliability analyses, particularly under seismic loading conditions.

Parallel to Bayesian approaches, Monte Carlo methods have also been extensively developed, aiming to reduce computational costs and improve efficiency in uncertainty analysis [19]. Among the commonly used techniques are Multilevel Monte Carlo (MLMC) [20], which relies on a hierarchy of simulations with varying accuracy, and Multifidelity Monte Carlo (MFMC) [21, 22], which combines models of different fidelity levels. More specialized variants have also emerged, such as Multicanonical Sequential Monte Carlo (MSMC) [23], enabling the reconstruction of full variable distributions while accounting for rare events, and Enhanced Monte Carlo (EMC) [24], which improves the accuracy of confidence interval estimation and reduces uncertainty overestimation. A practical example is provided by the work of Zanoni et al. [25], who proposed improved MFMC estimators employing dimensionality reduction techniques to enhance correlation between high and low-fidelity models. This method allows MFMC to be applied even in cases where classical approaches fail due to inconsistent random parameters between models. Numerical experiments demonstrated that the proposed estimators exhibit lower variance and higher accuracy compared with both the standard Monte Carlo method and baseline MFMC versions.

Within non-probabilistic methods, approaches based on interval numbers have been intensively developed, enabling the modeling of uncertainty without requiring full knowledge of probability distributions. Variants include interval field formulations applied to boundary value problems in mechanics and engineering [26], interval uncertainty propagation methods integrated with deep neural networks for the analysis of aerospace structures [27], as well as approaches based on interval fields that allow for spatial uncertainty representation in geotechnical engineering under limited measurement data [28]. In this context, Gong et al. [29] proposed a credible interval analysis, in which intervals and ellipsoids are assigned a specific level of credibility. This approach helps to address the typical underestimation of uncertainty in classical interval methods, while simultaneously improving the interpretability of results. The authors also implemented an adaptive Kriging-based metamodel (EAK), which enabled efficient estimation of dynamic structural responses, as demonstrated through

examples involving a mass–spring–damper system and selected aerospace components.

Alongside interval-based methods, fuzzy set–based approaches are also being actively developed and have found wide application in various engineering problems. Several variants utilize extended theoretical frameworks such as type-2 fuzzy sets or multi-fuzzy sets, which enhance flexibility in representing complex sources of uncertainty [30], as well as hybrid solutions that integrate fuzzy logic with machine learning methods, particularly in the context of environmental engineering and sustainable development [31]. For example, Xu et al. [32] proposed a Bayesian inference framework based on type-2 fuzzy sets and a cloud model, which enables the simultaneous representation of epistemic and linguistic uncertainty in the risk analysis of engineering systems. The authors demonstrated that integrating fuzzy sets with probabilistic reasoning allows for a more realistic risk assessment in situations of data scarcity, as confirmed through examples involving energy infrastructure and the chemical industry.

A new direction of development involves approaches that integrate interval numbers and fuzzy sets. A key example of this approach are Asymmetric Interval Numbers [4], which are demonstrated in this paper through selected engineering case studies.

3. Methods

This section is devoted to recalling the primary concepts of interval numbers used throughout this analysis. We begin by summarizing the properties of CINs before detailing the theoretical foundations of AINs, a generalization that allows for a different representation of uncertainty. The definitions and arithmetic framework for AINs are recalled from the work [4].

3.1 Classical Interval Numbers

Classical Interval Analysis provides a straightforward approach to address data uncertainty [3]. A Classical Interval Number represents an uncertain quantity X as a closed interval $[a, b]$ defined as:

$$X = [a, b] = \{x \in R \mid a \leq x \leq b\} \tag{1}$$

In this framework, any value between the infimum a and the supremum b is considered equally probable. This corresponds to a uniform probability density function (PDF) and a cumulative distribution function (CDF).

$$\text{pdf}(x) = \begin{cases} \frac{1}{b-a}, & a \leq x \leq b \\ 0, & \text{otherwise} \end{cases} \tag{2}$$

$$\text{cdf}(x) = \begin{cases} 0, & x < a, \\ \dfrac{x-a}{b-a}, & a \leq x \leq b, \\ 1, & x > b. \end{cases} \tag{3}$$

A key characteristic of a CIN is its midpoint, calculated as $\text{mid}(X) = (a + b)/2$. This value serves as the central point of the interval and reflects the underlying assumption of a symmetric distribution of uncertainty.

3.2 Asymmetric Interval Numbers

Asymmetric Interval Numbers were introduced to enhance the modeling of uncertainty by incorporating the expected value directly within the interval's representation, combining the ease of iden-

tification of classical intervals with a more advanced capability for modeling uncertainty.

An AIN is formally defined as a closed interval number $[a, b]$ with a given characteristic value c, where c represents the expected value $E(X)$. The formal notation is:

$$X = [a, b]_c = \{x \in R \mid a \leq x \leq b \wedge c = E(X)\} \tag{4}$$

This formulation assumes that the probability distribution is described by two distinct uniform densities, α and β, over the sub-intervals $[a, c]$ and $[c, b]$, respectively. The probability density function for an AIN is given by:

$$\text{pdf}(x) = \begin{cases} \alpha, & a \leq x < c, \\ \beta, & c \leq x \leq b, \\ 0, & \text{otherwise.} \end{cases} \tag{5}$$

The values for the densities α and β are uniquely determined based on the density normalization theorem and the definition of the expected value, resulting in the following expressions:

$$\alpha = \frac{b - c}{(b - a)(c - a)}; \quad \beta = \frac{c - a}{(b - a)(b - c)} \tag{6}$$

3.3 Arithmetic Operations on AINs

The arithmetic for AINs extends classical interval operations by defining how the expected value propagates through calculations. For non-linear transformations, the expected value of the resulting AIN is calculated using the Law of the Unconscious Statistician (LOTUS). For two AINs, $X = [a_1, b_1]_{c_1}$ and $Y = [a_2, b_2]_{c_2}$, the fundamental operations are defined as follows:

I. Addition:

$$X + Y = [a_1, b_1]_{c_1} + [a_2, b_2]_{c_2} = [a_1 + a_2,\ b_1 + b_2]_{c_1 + c_2} \tag{7}$$

II. Subtraction:

$$X - Y = [a_1, b_1]_{c_1} - [a_2, b_2]_{c_2} = [a_1 - b_2,\ b_1 - a_2]_{c_1 - c_2} \tag{8}$$

III. Multiplication:

$$\begin{aligned} X \cdot Y = [a_1, b_1]_{c_1} \cdot [a_2, b_2]_{c_2} = \\ [\min\{a_1a_2,\ a_1b_2,\ b_1a_2,\ b_1b_2\},\ \max\{a_1a_2,\ a_1b_2,\ b_1a_2,\ b_1b_2\}]_{c_1c_2} \end{aligned} \tag{9}$$

IV. Division:

$$\begin{aligned} X \div Y = [a_1, b_1]_{c_1} \div [a_2, b_2]_{c_2} = \\ \left[\min\left\{\frac{a_1}{a_2}, \frac{a_1}{b_2}, \frac{b_1}{a_2}, \frac{b_1}{b_2}\right\},\ \max\left\{\frac{a_1}{a_2}, \frac{a_1}{b_2}, \frac{b_1}{a_2}, \frac{b_1}{b_2}\right\}\right]_{c_3} \end{aligned} \tag{10}$$

where

$$c_3 = \begin{cases} c_1 \cdot \left(\alpha \cdot \ln\left(\dfrac{c_2}{a_2}\right) + \beta \cdot \ln\left(\dfrac{b_2}{c_2}\right)\right), & a_2 \neq b_2, \\ c_1 \div c_2, & a_2 = b_2 \end{cases} \tag{11}$$

V. Square root (for $a \geq 0$):

$$\sqrt{[a, b]_c} = [\sqrt{a},\ \sqrt{b}]_{c_2} \tag{12}$$

where c_2 is determined based on LOTUS.

$$c_2 = \begin{cases} \frac{2}{3}\left(\alpha(c^{1.5} - a^{1.5}) + \beta(b^{1.5} - c^{1.5})\right), & a \neq b, \\ \sqrt{c}, & a = b \end{cases} \tag{13}$$

VI. Exponentiation:

$$([a, b]_c)^n = [a^n,\, b^n]_{c_2} \tag{14}$$

$$c_2 = \begin{cases} \frac{1}{n+1}\left(\alpha(c^{n+1} - a^{n+1}) + \beta(b^{n+1} - c^{n+1})\right), & a \neq b, \\ c^n, & a = b \end{cases} \tag{15}$$

where power exponent $n \neq -1$ and $a \geq 0$.

To quantify the distributional properties of an AIN, an asymmetry coefficient A is introduced, where $A \in (-1, 1)$. The coefficient provides a direct measure of the asymmetry level of the AIN distribution. It is defined for $X = [a, b]_c$ as follows:

$$A = \begin{cases} \frac{a+b-2c}{b-a}, & a \neq b \\ 0, & a = b \end{cases} \tag{16}$$

The value of the coefficient is zero for a symmetric distribution, negative for distributions that exhibit left-sided asymmetry (where the probability of an event in $[a, c]$ is lower than in $[c, b]$), and positive for distributions that show right-sided asymmetry.

4. Engineering Case Studies

To demonstrate the practical applicability and advantages of Asymmetric Interval Numbers in engineering analysis, three case studies were conducted. Section 4.1 presents an analysis of renewable energy production in a wind farm, Section 4.2 focuses on the estimation of structural loads under extreme weather conditions, and Section 4.3 investigates the complexities of aerodynamic interactions between wind turbines. In each of these cases, we model system parameters using both CINs and AINs to provide a direct comparison. The calculations involving AINs were performed using the `AsymIntervals` Python library [9], which provides a robust and validated framework for arithmetic and probabilistic operations on asymmetric intervals. A key aspect of our methodology is to ensure a fair comparison. Therefore, the initial input parameters for AINs are defined with an expected value equal to the midpoint of their respective intervals. This initial symmetry allows us to isolate and quantify the asymmetry induced solely by the non-linear relationships within the engineering models themselves. The primary goal is to compare the expected value $E(X)$ from the AIN approach with the midpoint from the CIN approach, showing that the AIN result offers a more realistic and physically consistent measure of central tendency.

4.1 Estimation of Annual Energy Production in a Wind Farm

The first case study focuses on estimating the total annual energy production (E_{year}) for an offshore wind farm consisting of $N = 50$ turbines. Accurate estimation of energy yield is an essential task for both technical and financial planning of renewable energy projects. The process is subject to significant uncertainty due to fluctuating atmospheric conditions, natural variations in the efficiency

of the turbine components, and operational strategies. Our objective is to model these uncertainties to produce a more realistic energy forecast [33, 34].

The instantaneous power generated by a single turbine is a non-linear function of several variables, described by the formula [35]:

$$P(v) \;=\; \frac{1}{2}\,\rho\,A\,C_p\,v^3\,\eta \tag{17}$$

The total annual energy is calculated as

$$E_{\text{year}} \;=\; P_{\text{avg}} \cdot N \cdot 8760\ \text{h} \tag{18}$$

where P_{avg} is the average power of a single turbine, and 8760 corresponds to the number of hours in a year.

The uncertain input parameters, modeled as both CINs and AINs, are detailed in Table 1.

Table 1
Input parameters for the wind farm energy production model

Parameter	Symbol	Interval	Initial Exp. Value (c)	Unit
Air Density	ρ	$[1.20,\ 1.25]$	1.225	kg/m^3
Rotor Diameter	D	$[118,\ 122]$	120	m
Power Coefficient	C_p	$[0.40,\ 0.50]$	0.45	—
Wind Speed	v	$[6.50,\ 9.50]$	8.0	m/s
Efficiency	η	$[0.85,\ 0.95]$	0.90	—

Using the `AsymIntervals` library, the uncertainty from the parameters in Table 1 was propagated through Equation (17). First, the interval for the rotor area $A = \pi D^2/4$ was calculated, and subsequently, all intervals were combined to find the total annual energy production. The final estimates are presented and compared with the classical interval approach in Table 2.

Table 2
Comparison of annual energy production estimates

Method	Interval Bounds [GWh]	Expected Value [GWh]	Asymmetry Coeff.
CIN	[268.3, 1303.3]	Midpoint: 785.8	0.0
AIN	[268.3, 1303.3]	**Exp. Value: 651.3**	**0.259**

A significant discrepancy is observed between the central estimates derived from the two methods. The expected value obtained with AINs (651.3 GWh) represents a substantial downward shift of approximately 17% compared to the CIN midpoint (785.8 GWh). This difference is a direct consequence of the strong cubic non-linearity ($P \sim v^3$) in the power equation. While a classical interval's midpoint implicitly assumes a symmetric output, the cubic relationship disproportionately amplifies the effect of values from the lower end of the input parameter ranges. This non-linearity shifts the probability-weighted average toward lower energy outcomes. This induced asymmetry is visually represented in Fig. 1, which shows the probability density function of the resulting AIN. The plot clearly illustrates that the probability density is significantly higher in the lower portion of the interval compared to the upper portion. The blue dashed line marks the expected value, which is the center of mass of the distribution, while the red dashed line indicates the traditional midpoint. The quantitative difference between these two points, approximately 134.5 GWh, highlights the significant skew captured by the AIN model.

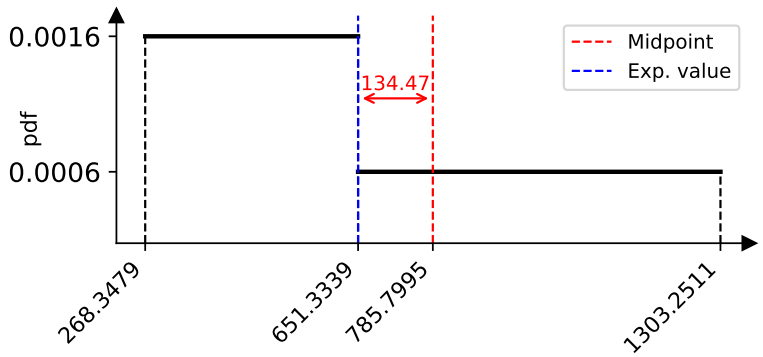

Fig. 1. Probability Density Function of the AIN for annual energy production.

To demonstrate that this asymmetry is not just a theoretical curiosity but a measurable improvement in analytical accuracy, let's consider a practical application. Suppose an investor or operator wants to estimate the probability that the annual energy production will fall below a critical threshold of 700 GWh, which might represent a break-even point.

Using the CIN approach, which assumes a uniform probability distribution across the entire interval [268.3, 1303.3] GWh, the probability $P_{CIN}(X < 700) \approx 41.7\%$.
Using the AIN model, we use its two-level PDF shown in Fig. 1. The probability is the total area under the curve up to 700 GWh $P_{AIN}(X < 700) \approx 65.8\%$.

The AIN model suggests a 65.8% chance of production being below 700 GWh, whereas the traditional CIN model suggests only a 41.7% chance. The 24% discrepancy in probability estimates highlights the practical importance of accounting for asymmetry in non-linear systems. In the context of wind farm planning, this difference directly affects investment risk assessment and operational forecasts, demonstrating the value of AIN over classical interval methods for energy production modeling.

4.2 Estimation of Storm Wind Load on a Turbine Tower

In this case study, we investigate the wind pressure force F_w acting on a turbine tower of height $H \in [85,\ 95]$m during an extreme storm event. The tower is assumed to operate in offshore conditions, where exposure to high and rapidly varying wind speeds represents a significant design challenge. During extreme storms, offshore wind turbines are exposed to extreme environmental loads that directly affect their safety and reliability, while the combined action of wind and waves introduces additional cyclic stresses influencing structural fatigue [36, 37]. Accurate estimation of storm-induced wind loads remains essential, as such events can generate excessive aerodynamic forces that may even require turbine shutdowns [38]. The aim of this study is to capture the effect of the nonlinearity ($F \sim v^2$) on the shift of the expected value relative to the interval midpoint.

The wind pressure force acting on the tower is described by the formula [39]:

$$F_w(v) \ = \ \frac{1}{2}\,\rho\, C_d\, A_f\, v^2, \tag{19}$$

The uncertain input parameters for the wind load estimation model are detailed in Table 3.

Table 3
Input parameters for the storm wind load model

Parameter	Symbol	Interval	Initial Exp. Value (c)	Unit
Air Density	ρ	$[1.20,\ 1.25]$	1.225	kg/m^3
Drag Coefficient	C_d	$[1.10,\ 1.30]$	1.20	—
Projected Area	A_f	$[250,\ 300]$	275	m^2
Wind Speed	v	$[40,\ 55]$	47.5	m/s

The propagation of these uncertainties through Equation (19) was performed using the `AsymIntervals` library, resulting in the corresponding interval estimate for the wind load. A comparative analysis of the CIN and AIN estimates is provided in Table 4.

Table 4
Comparison of storm wind load estimates

Method	Interval Bounds [kN]	Expected Value [kN]	Asymmetry Coeff.
CIN	[264.0, 737.3]	Midpoint: 500.7	0.0
AIN	[264.0, 737.3]	Exp. Value: 459.8	0.173

The AIN model's expected value (459.8 kN) is 8.2% lower than the CIN midpoint (500.7 kN). This discrepancy arises directly from the v^2 term in the equation, an effect the symmetric CIN model cannot capture.

To demonstrate the practical significance, let's consider a design engineer's perspective. Using the classical interval, an engineer might base the preliminary design on the midpoint value of 500.7 kN, treating it as the most representative load. However, the AIN analysis reveals that the physically-weighted average force is actually 459.8 kN.

This insight shows that a design based on the CIN midpoint would be over-dimensioned by approximately 8.2% on average. While safety margins are crucial, systemic overestimation driven by flawed modeling leads to unnecessary material usage and increased costs, especially when scaled across an entire wind farm.

4.3 Estimation of Power Output with Wake Effect Between Two Wind Turbines

This case study examines the total power output of two offshore wind turbines arranged in a series, separated by a distance $x = 7D$, where $D = 120$ m is the rotor diameter. An important factor in wind farm performance is the aerodynamic wake effect, where the upstream turbine creates a shadow of turbulent, lower-velocity wind, reducing the energy available to the downstream turbine. This analysis aims to quantify the total power output uncertainty, focusing on how the cubic non-linearity of power generation ($P \sim v^3$) is amplified by the wake effect.

To model the velocity deficit, we use the Jensen wake model [40]. The wind speed v_1 behind the first turbine is described by the equation:

$$v_1 = v_0 \left(1 - \frac{2a}{(1 + 2k\frac{x}{D})^2}\right) \tag{20}$$

where v_0 is the initial wind speed, a is the axial induction factor, and k is the wake decay constant. The power output of each turbine is then calculated using Equation (17).

The uncertain input parameters for both the wake model and the power equation are detailed in Table 5.

Table 5
Input parameters for the wake effect and power production model

Parameter	Symbol	Interval	Initial Exp. Value (c)	Unit
Initial Wind Speed	v_0	$[8.0,\ 10.0]$	9.0	m/s
Axial Induction Factor	a	$[0.28,\ 0.32]$	0.30	—
Wake Decay Constant	k	$[0.04,\ 0.06]$	0.05	—
Air Density	ρ	$[1.20,\ 1.25]$	1.225	kg/m^3
Power Coefficient	C_p	$[0.44,\ 0.50]$	0.47	—
Efficiency	η	$[0.88,\ 0.94]$	0.91	—

First, the power output for the upstream turbine (P_1) and the downstream turbine (P_2) were calculated separately. The total power ($P_{total} = P_1 + P_2$) was then determined by summing their respective interval representations using AIN. A comparative analysis of the total power estimates from the CIN and AIN approaches is presented in Table 6.

Table 6
Comparison of storm wind load estimates

Method	Interval Bounds [MW]	Expected Value [MW]	Asymmetry Coeff.
CIN	[1.88, 5.25]	Midpoint: 3.57	0.0
AIN	[1.88, 5.25]	Exp. Value: 3.29	0.167

The analysis shows that the expected value from the AIN model (3.29 MW) is approximately 7.8% lower than the midpoint of the classical interval (3.57 MW). This significant downward shift is caused by the compounding effect of the cubic relationship ($P \sim v^3$). Even small reductions in wind speed due to the wake effect lead to substantial drops in power output, a phenomenon that skews the probability distribution of the total output towards lower values.

This asymmetry is visualized in Fig. 2, which displays PDF for the total power output. The higher probability density in the lower end of the interval is evident. The difference between the traditional midpoint and the more realistic expected value is approximately 0.28 MW, highlighting the substantial modeling error introduced by the CIN approach.

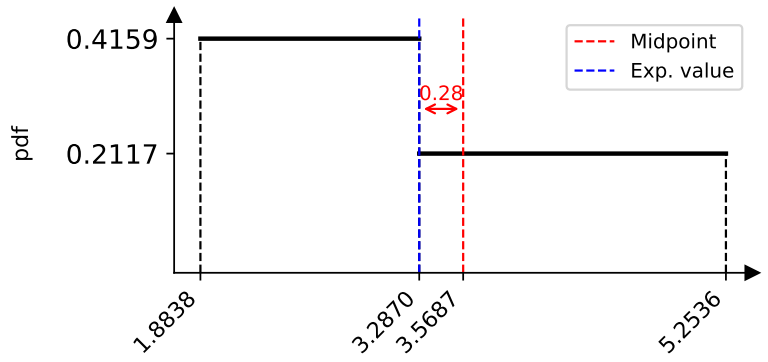

Fig. 2. Probability Density Function of the AIN for total power output with wake effect.

To illustrate the practical significance of this distinction, consider a scenario in which a wind farm operator is contractually obliged to provide at least 3.5 MW of power to the grid. The probability of failing to meet this target, $P(X < 3.5)$, can be estimated using two different representations of uncertainty. Under the CIN approach, which assumes a uniform distribution of possible outcomes, the probability that the output being below 3.5 MW is $P_{CIN}(X < 3.5) \approx 48.1\%$. In contrast, the AIN

model accounts for the skewed nature of the probability distribution. Based on its two-level probability density function, the estimated probability is $P_{AIN}(X < 3.5) \approx 62.9\%$.

The difference of 14.8 percentage points suggests that the AIN model may better capture operational risk in cases where uncertainty exhibits an asymmetric pattern. In practice, this approach reflects the fact that power generation uncertainty is rarely evenly distributed, as lower outputs are often more likely than higher outputs due to technical, environmental, or stochastic factors. Moreover, the inherent asymmetry of arithmetic operations represents an important computational challenge, as it requires maintaining consistency between the direction of uncertainty and the propagation of error through subsequent calculations. Consequently, relying solely on the CIN model could lead to an underestimation of the probability of non-delivery, resulting in overly optimistic forecasts and insufficient risk mitigation measures. The AIN model therefore offers a potentially more informative representation, enabling a more nuanced assessment of risk in energy management and reliability analysis.

5. Conlusions

This work applies Asymmetric Interval Numbers to selected engineering problems, demonstrating their usefulness as a practical extension of classical interval numbers. While CINs assume symmetric uncertainty, AINs enable independent treatment of deviations on both sides of the central value, which more accurately reflects real-world measurement errors, technological variations, and nonlinear effects. Using the `AsymIntervals` library, three case studies were analyzed. These include the estimation of annual wind farm energy production, the assessment of storm wind loads on a turbine tower, and the evaluation of power output under wake effects.

The obtained results consistently showed that AINs provide more realistic expected values compared to CINs, capturing asymmetries that significantly influence both technical assessments and decision-making processes. In the case of wind energy production, the method offered more reliable estimates of output variability, directly supporting investment and operational planning. For storm-induced structural loads, AIN allowed for a more accurate evaluation of risks while avoiding excessive over-dimensioning of structures. Finally, in the analysis of wake effects, the method revealed hidden asymmetries in power distribution that classical intervals failed to capture, underlining the importance of considering asymmetric uncertainty in nonlinear aerodynamic models.

In summary, the presented case studies confirm that the application of AIN leads to more stable, interpretable, and practically relevant outcomes in engineering analyses. At the same time, the findings highlight the potential of extending this approach to a wider range of problems where uncertainty plays a decisive role. Future research should therefore focus on applying AINs to additional engineering domains.

References

[1] Shi, Y., Wei, P., Feng, K., Feng, D.-C., & Beer, M. (2025). A survey on machine learning approaches for uncertainty quantification of engineering systems. *Machine Learning for Computational Science and Engineering*, *1*(1), 11. https://doi.org/10.1007/s44379-024-00011-x

[2] Chen, Y., Shi, J., & Yi, X.-J. (2021). Design improvement for complex systems with uncertainty. *Mathematics*, *9*(11), 1173. https://doi.org/10.3390/math9111173

[3] Moore, R. E., Kearfott, R. B., & Cloud, M. J. (2009). *Introduction to interval analysis*. SIAM. https://doi.org/10.1137/1.9780898717716

[4] Sałabun, W. (2025a). Asymmetric interval numbers: A new approach to modeling uncertainty. *Fuzzy Sets and Systems*, *499*, 109169. https://doi.org/10.1016/j.fss.2024.109169

[5] Landowski, M. (n.d.). Differences between moore and rdm interval arithmetic. *Intelligent Systems' 2014: Proceedings of the 7th IEEE International Conference Intelligent Systems IS'2014, September 24-26, 2014, Warsaw, Poland, Volume 1: Mathematical Foundations, Theory, Analyses*, 331–340. https://doi.org/10.1007/978-3-319-11313-5_30

[6] Sahlin, E., & Magnusson, B. (2022). Expression for uncertainty intervals handling skewness when the relative standard uncertainty is independent of the measurand level. *Accreditation and Quality Assurance*, *27*(4), 223–233. https://doi.org/10.1007/s00769-022-01506-x

[7] Xiaojing, W., Pengcheng, D., Lichao, Y., Zhengping, Z., & Fei, Z. (2023). Uncertainty analysis of measured geometric variations in turbine blades and impact on aerodynamic performance. *Chinese Journal of Aeronautics*, *36*(6), 140–160. https://doi.org/10.1016/j.cja.2023.03.041

[8] Uhlig, S., Colson, B., & Gowik, P. (2023). Measurement uncertainty interval in case of a known relationship between precision and mean. *F1000Research*, *12*, 996. https://doi.org/10.12688/f1000research.139111.1

[9] Sałabun, W. (2025b). Asymintervals: A python library for uncertainty modeling with asymmetric interval numbers. *SoftwareX*, *32*, 102380. https://doi.org/10.1016/j.softx.2025.102380

[10] Riedmaier, S., Danquah, B., Schick, B., & Diermeyer, F. (2021). Unified framework and survey for model verification, validation and uncertainty quantification. *Archives of Computational Methods in Engineering*, *28*(4). https://doi.org/10.1007/s11831-020-09473-7

[11] Romero, V. J. (2024). A systems approach to effective treatment of aleatory and epistemic uncertainties involving typical information limitations in engineering projects. *AIAA SCITECH 2024 Forum*, 0791. https://doi.org/10.2514/6.2024-0791

[12] Hasan, K. N., Preece, R., & Milanović, J. V. (2019). Existing approaches and trends in uncertainty modelling and probabilistic stability analysis of power systems with renewable generation. *Renewable and Sustainable Energy Reviews*, *101*, 168–180. https://doi.org/10.1016/j.rser.2018.10.027

[13] Hakami, A. M., Hasan, K. N., Alzubaidi, M., & Datta, M. (2022). A review of uncertainty modelling techniques for probabilistic stability analysis of renewable-rich power systems. *Energies*, *16*(1), 112. https://doi.org/10.3390/en16010112

[14] Aien, M., Hajebrahimi, A., & Fotuhi-Firuzabad, M. (2016). A comprehensive review on uncertainty modeling techniques in power system studies. *Renewable and Sustainable energy reviews*, *57*, 1077–1089. https://doi.org/10.1016/j.rser.2015.12.070

[15] Pasparakis, G. D., Graham-Brady, L., & Shields, M. D. (2025). Bayesian neural networks for predicting uncertainty in full-field material response. *Computer Methods in Applied Mechanics and Engineering*, *433*, 117486. https://doi.org/10.1016/j.cma.2024.117486

[16] Abulawi, Z., Hu, R., Balaprakash, P., & Liu, Y. (2025). Bayesian optimized deep ensemble for uncertainty quantification of deep neural networks: A system safety case study on sodium fast reactor thermal stratification modeling. *Reliability Engineering & System Safety*, 111353. https://doi.org/10.1016/j.ress.2025.111353

[17] Ochella, S., Dinmohammadi, F., & Shafiee, M. (2024). Bayesian neural networks for uncertainty quantification in remaining useful life prediction of systems with sensor monitoring. *Advances in Mechanical Engineering*, *16*(7), 16878132241239802. https://doi.org/10.1177/16878132241239802

[18] Kurumbhati, M., Ramancha, M., Aakash, B., Conte, J., & Lotfizadeh, K. (2024). Hierarchical bayesian modeling for calibration and uncertainty quantification of constitutive material models: Application to a uniaxial steel material model. *Engineering Structures*, *318*, 118409. https://doi.org/10.1016/j.engstruct.2024.118409

[19] Zhang, J. (2021). Modern monte carlo methods for efficient uncertainty quantification and propagation: A survey. *Wiley Interdisciplinary Reviews: Computational Statistics*, *13*(5), e1539. https://doi.org/10.1002/wics.1539

[20] Giles, M. B. (2008). Multilevel monte carlo path simulation. *Operations research*, *56*(3), 607–617. https://doi.org/10.1287/opre.1070.0496

[21] Ng, L. W., & Willcox, K. E. (2014). Multifidelity approaches for optimization under uncertainty. *International Journal for numerical methods in Engineering*, *100*(10), 746–772. https://doi.org/10.1002/nme.4761

[22] Peherstorfer, B., Willcox, K., & Gunzburger, M. (2016). Optimal model management for multifidelity monte carlo estimation. *SIAM Journal on Scientific Computing*, *38*(5), A3163–A3194. https://doi.org/10.1137/15M1046472

[23] Millar, R., Li, H., & Li, J. (2023). Multicanonical sequential monte carlo sampler for uncertainty quantification. *Reliability Engineering & System Safety*, *237*, 109316. https://doi.org/10.1016/j.ress.2023.109316

[24] Anyfantis, K. N. (2025). Optimizing uncertainty estimation in enhanced monte carlo methods. *Structural Safety*, 102617. https://doi.org/10.1016/j.strusafe.2025.102617

[25] Zanoni, A., Geraci, G., Salvador, M., Menon, K., Marsden, A. L., & Schiavazzi, D. E. (2024). Improved multifidelity monte carlo estimators based on normalizing flows and dimensionality reduction techniques. *Computer Methods in Applied Mechanics and Engineering*, *429*, 117119. https://doi.org/10.1016/j.cma.2024.117119

[26] Hu, H., Wu, Y., Batou, A., & Ouyang, H. (2023). Uncertainty propagation with b-spline based interval field decomposition method in boundary value problems. *Applied Mathematical Modelling*, *123*, 159–177. https://doi.org/10.1016/j.apm.2023.06.007

[27] Yan, S., & Michael, B. (2024). Deep learning-driven interval uncertainty propagation for aeronautical structures. *Chinese Journal of Aeronautics*, *37*(12), 71–86. https://doi.org/10.1016/j.cja.2024.05.009

[28] Feng, C., Broggi, M., Hu, Y., Faes, M. G., & Beer, M. (2025). Interval fields for geotechnical engineering uncertainty analysis under limited data. *ASCE-ASME Journal of Risk and Uncertainty in Engineering Systems, Part A: Civil Engineering*, *11*(2), 04025004. https://doi.org/10.1061/AJRUA6.RUENG-1467

[29] Gong, J., Wang, X., & Lv, T. (2023). A credible interval analysis method for uncertain structures under nonprobabilistic framework. *Computer Methods in Applied Mechanics and Engineering*, *404*, 115833. https://doi.org/10.1016/j.cma.2022.115833

[30] Kannan, J., Jayakumar, V., Kausar, N., Pamucar, D., & Simic, V. (2024). Enhancing decision-making with linear diophantine multi-fuzzy set: Application of novel information measures in medical and engineering fields. *Scientific Reports*, *14*(1), 28537. https://doi.org/10.1038/s41598-024-79725-0

[31] Bressane, A., Garcia, A. J. d. S., Castro, M. V. d., Xerfan, S. D., Ruas, G., & Negri, R. G. (2024). Fuzzy machine learning applications in environmental engineering: Does the ability to deal with uncertainty really matter? *Sustainability*, *16*(11), 4525. https://doi.org/10.3390/su16114525

[32] Xu, J., Sui, Y., Yu, T., Ding, R., Dai, T., & Zheng, M. (2024). A new fuzzy bayesian inference approach for risk assessments. *Symmetry*, *16*(7), 786. https://doi.org/10.3390/sym16070786

[33] Yan, J., Liu, Y., Han, S., Wang, Y., & Feng, S. (2015). Reviews on uncertainty analysis of wind power forecasting. *Renewable and Sustainable Energy Reviews*, *52*, 1322–1330. https://doi.org/10.1016/j.rser.2015.07.197

[34] Kumar, K. P., & Saravanan, B. (2017). Recent techniques to model uncertainties in power generation from renewable energy sources and loads in microgrids–a review. *Renewable and Sustainable Energy Reviews*, *71*, 348–358. https://doi.org/10.1016/j.rser.2016.12.063

[35] Manwell, J. F., McGowan, J. G., & Rogers, A. L. (2010). *Wind energy explained: Theory, design and application*. John Wiley & Sons. https://doi.org/10.1002/9781119994367

[36] Wang, L., Zhou, W., Guo, Z., & Rui, S. (2020). Frequency change and accumulated inclination of offshore wind turbine jacket structure with piles in sand under cyclic loadings. *Ocean Engineering*, *217*, 108045. https://doi.org/10.1016/j.oceaneng.2020.108045

[37] Charlton, T., & Rouainia, M. (2022). Geotechnical fragility analysis of monopile foundations for offshore wind turbines in extreme storms. *Renewable Energy*, *182*, 1126–1140. https://doi.org/10.1016/j.renene.2021.10.092

[38] Das, K., Guo, F., Nuño, E., & Cutululis, N. A. (2020). Frequency stability of power system with large share of wind power under storm conditions. *Journal of Modern Power Systems and Clean Energy*, *8*(2), 219–228. https://doi.org/10.35833/MPCE.2018.000433

[39] Moebs, W., Ling, S. J., & Sanny, J. (2016). *University physics volume 1* [Accessed: 2025-10-19]. OpenStax. https://openstax.org/books/university-physics-volume-1/pages/6-4-drag-force-and-terminal-speed

[40] Jensen, N. O. (1983). *A note on wind generator interaction*. Risø National Laboratory. https://orbit.dtu.dk/en/publications/a-note-on-wind-generator-interaction